CHAPTER 5

EVALUATION OF EFFICIENT STACKING OF AROMATIC RINGS IN THE INTERCALATION BETWEEN AZA-ANALOGUES OF ACRIDINE-4-CARBOXAMIDES AND BASE PAIRS OF DNA

SUMMARY

The intercalation of the chromophore of azaacridinecarboxamide, having different substituents, with base pairs of DNA has been studied by *ab initio*, DFT and MP2 level of theories. The results obtained from this calculation shows variation in interaction energies with respect to substituents. The chromophores with substituents -CO,-NH_2 and -Cl interacts favourably with GC sequence, and the stacking of -CO substituted chromophore is more than the - NH_2 and -Cl substituted chromophore.

5.1 INTRODUCTION

Many acridine-4-carboxamides formed by modifying the chromophore (acridine ring) with substituents have been reported in the search of highly potent anticancer drugs. In this context the correlation between DNA intercalation by chromophore and cytotoxic potency are normally examined ***[1-10]***. A comparative study on intercalation ability of drugs within DNA base pair and their biological properties have been determined to extract information for designing new drugs.

We know that the aromatic chromophores generally show slight preference for GC sequences and produce changes in the helix unwinding angle after intercalation ***[9-15]***. As such carbonyl containing chromophores bind most strongly than other chromophores having different substituents. On the other hand conformation of chromophore also affects the intercalative mode of binding in drug DNA complex. Generally the planar chromophores are preferred for intercalation than other non-planar chromophore. It has been noted that non-intercalative drug are 2000 fold less potent than intercalative drugs like 9-aminoacridine-4-carboxamide ***[16-17]***. So the extent of intercalative binding may correlate with potency of drug.

A comparative study on the intercalative binding ability of drugs within DNA

sequences and their biological properties have been carried out to extract some information useful for designing new drugs. The substituents having different electronic properties such as -C=O, -Cl and -NH_2 have been used for modifying chromophore.

In this study we report the evaluation of stacking ability of azaacridine-4-carboxamides having different substituents in chromophore. Here for monitoring intercalative mode of binding we have taken several structures for each drug by changing the position of Nx in aromatic ring (four different position of Nx), and 32 stacked models of Drug-DNA base pair stacking were constructed for the drug with particular Nx position so that the dependence of stacking energies with substituents can be examined. We aim to study stacking of chromophore with base pairs by using *ab initio* and DFT method with various basis set.

5.2 METHODOLOGY

The stacked structures of substituted azaacridine-4-carboxamides with AT and GC sequences were constructed by keeping drugs over base pair at a separation of 3.6Å (**Figure 5.1**). All the possible stacked structures (32 per Nx position per substituents) are modeled for examining π–π and σ–π interactions for a drug having particular Nx position (**Figure 5.2-5.4**). Three substituents were considered to examine the electronic effect on Nx. The drug and DNA sequences were completely optimized with 6-31G basis set, and the stacked models were constructed from the optimized molecular fragment of drug and base sequences. We further extended higher level calculations with the use of 6-31G** for the most favorable stacked structures. We know that intermolecular correlation energies are not covered in the HF calculation unless MP2 level of calculation with large basis set is included, which is also the essential factor for computing dispersion forces operating in stacked structures ***[18]***. However the usefulness of less accurate *ab initio* and DFT methods has been observed ***[18]***. Indeed, some intramolecular correlation energies can be obtained from *ab initio* and DFT calculations. For such large molecular system 6-31G**/DFT method may still be useful for qualitative interpretation of sequence specificity of drug for DNA sequences. Hence we also carried out B3LYP/6-31G** calculation to estimate the stacking energies of optimum stacked structures of drug and base pair ***[19]***.

5.3 RESULTS AND DISCUSSION

5.3.1 Contribution of $\pi-\pi$ Interaction in chromophore and base pair stacking:

All stacked models formed between drug chromophore and sequences were constructed from the overlapping of chromophore along the axial direction of sequences (**Figure 5.1**). The stacking of aromatic rings of chromophore and AT sequences were studied ($\pi-\pi$ interactions), and the optimum structure of AT-Drugs are shown in **Figure 5.5a-l**. Again similar calculations were carried out for the stacking of drugs with GC sequences (**Figure 5.6a-l**). The plots of stacked models versus the interaction energies calculated with HF/6-31G route are shown in **Figure 5.9a-c** and **Figure 5.10a-c**, where the minimum interaction energies in the plot correspond to optimum stacked structures. The main reason for adopting this method is to examine any significant contribution from $\pi-\pi$ interactions in chromophore and sequence stacking in addition to the contribution of Nx. In all these models, there observed wide variation of stacking energies. It clearly indicates that the interaction of chromophore and base pair induces electron distribution leading to variation in stacking energies (**Table 5.2** and **5.3**). The optimum stacked structures for all chromophore having different Nx positions have been analysed and there observed shifting of chromophore along the sequences (**Figure 5.a-l, 5.6a-l, 5.7a-c** and **5.8a-c**).

The results obtained from AT and chromophore stacking can be interpreted in two ways-

(a) the $\pi-\pi$ stackings in all the models formed by modifying the substituents, and

(b) the $\pi-$ group stacking of substituents and aromatic rings of sequences.

In all the models the substituent effect is not negligible as observed from the stacking of drug having different substituents and Nx at different position. Among these various stacked models, as per the higher basis sets calculations, the stacking of 9-oxoaza(5)acridone-4-carboxamide, where Nx is located at position 5 in ring is found to be most favorable (stacking location - AT-AZO7-11, where ring-2 of AT base pair stacked over ring-C of drug, **Figure 5.5a** and **Table 5.7a-c**). Similarly the optimum stacked model of 9-oxoaza(8)acridone-4-carboxamide with GC is shown in **Figure 5.6d**, and the stacking energies are shown in **Table 5.8a-c**.

5.3.2 Contribution of π– group interaction and π–σ interaction:

To understand the π–group interaction in various stacked structures of substituted azaacridine-4-carboxamides, we have considered few positions in AT sequence where the substituents are allowed to overlap with the aromatic ring (**Figure 5.7a-c**). The stacking energies of some π-group stacked models are higher than the interaction between the aromatic rings (π–π) (**Table 5.2, 5.9, 5.10**). However the interaction model of π–group includes some π–π interaction due to partial stacking of aromatic rings, but the structures are less favourable than the fully overlapped models of these aromatic rings (**Table 5.9, 5.10**). The change in the stacking energy with the shifting of Nx is observed. In view of the differences in the optimum stacked models of chromophore and base pair obtained from π–π stacking, the contribution of Nx and N of aromatic ring in the stacked model of chromophore and base pair can be emphasized. In fact π-group interaction is less favored than π–π interaction. Similarly we have explored the optimum stacked structures of AT with chromophore of 9-oxoaza(5)acridone-4-carboxamides, 9-oxoaza(6)acridone-4-carboxamides, 9-oxoaza(7)acridone-4-carboxamides and 9-oxoaza(8)acridone-4-carboxamides having Nx atom at different positions. The plot between optimum structures having N at different positions in chromophore versus interaction energies are shown in **Figure 5.9a-c**. We have analysed the net charges of heavy atoms, particularly on Nx and N of chromophore within the stacked model, and their comparison with those in free counterparts are made.

We have extended similar calculations for stacked models of drugs with GC base pair (**Table 5.3**). Likewise, the π–π stacking interactions due to overlapping of aromatic rings are explored. The plot of stacked models versus interaction energies are shown in (**Figure 5.10a-c**) and the variation of the interaction energies are similar to those of AT-drug stacking. The change in the net charges on Nx of free and those in optimum stacked structures are given in **Table 5.4a-c, 5.5a-c** and **5.6a-c**. It reveals that the involvement of Nx within stacking region results some changes in the net charges. However when Nx is not within the stacking region then there observe no change in net charges. If we compare the optimum stacked models of 9-oxoazaacridone-4-chromophore having Nx at 5,6,7 and 8 positions with GC base pair, the minimum stacking energy is found in the stacked model having Nx at 8. The optimum π–π stacked model of 9-chloroazaacridine-4-carboxamide and 9-aminoazaacridine-4-carboxamide with GC occur where Nx is at position 5. Among

the π–π stacked models of 9-oxoaza(8)acridone-4-carboxamide, 9-chloroaza(5)acridine-4-carboxamide and 9-aminoaza(5)acridine-4-carboxamides with GC base pair are found to be most stable (**Table 5.8a-c, Figure 5.6a-l**).

For the quantitative interpretation of the interaction energies, it is extremely important to take proper account of the various levels of theories; the change in interaction energies from HF to MP2 that includes proper account of electron correlation required for studying intermolecular stacking problem. Here the analysis of these systems may be taken up with the combined investigations using quantum mechanical methods such as DFT and HF methods with proper basis sets. As we know that DFT method is not proper for taking up long range type stacking interaction but some amount of intramolecular electron correlation included in the calculation might be useful. We encountered useful applicability of this method in taking up large molecular system where the feasibility of high level calculation is not possible. Here both DFT and HF/6-31G** stacking energies are obtained only for the optimum stacked models (**Table 5.7a-c** and **5.8a-c**). The interaction energies of these methods show some optimum stacked configurations but in some cases the results obtained from these methods vary. Hence the most stable stacked structures of drug and base pairs are found to be contributed from the accommodation of heavy atoms within the π–π interaction region (**Figures 5.5a-l** and **5.6a-l**). Alternatively, various stacked models are constructed in a manner such that the substituents (groups) stack with the aromatic ring of base pairs. The interaction energies are computed for these models at different level of theory so that the energy values emerge out of the concepts included in the various methods may be differentiated. Among the GC stacked structures of 9-oxoazaacridone-4-carboxamide, the most preferred stacking is found to be GC-AZO8-9 (**Table 5.8a**) where more **N** atoms found within the stacked region (**Figure 5.6d**). Similarly in the optimum stacked structures of -NH_2 substituted carboxamides, and the GC-AZN5-6 corresponds to minimum energy (**Table 5.8b**) and accommodation of heavy atoms (**N**) within the stacked region is noticed (**Figure 5.6e**). Similarly for 9-chloroazaacridine-4-carboxamides (GC-AZCl5-8), is the most stable structure is shown in **Figure 5.6l** (**Table 5.8c**)

Similar investigations have been carried out for >CO, -NH_2 and -Cl substituted carboxamides with AT sequences and the models corresponding to the minimum energies are AT-AZO5-11, AT-AZN7-6 and AT-AZCl7-6 (**Figures 5.5a, 5.5g, 5.5k** and **Table 5.7a-c**).

As we can see that the variation of interaction energies are small among these models, however, it is necessary to evaluate such stacking interaction before investigating the torsion of nucleic acid backbone as a result of interaction.

Now we can analyze the interaction energies in terms of the different level of calculations so that the primary factor operating in the stabilization of stacked structures may be elucidated based on the theory and any erroneous prediction encountered in the calculation. Starting from the crystallographic structure of drug-DNA complexes to the geometrical feature represented by theoretical method, one can easily make out that constructed stacked models are taken only for the overlapping of aromatic rings without considering the torsional force of DNA backbone that may be distorted after intercalation. In the sense that sugar conformation might be disrupted after intercalation by drugs with sequences of DNA. The twisting or unwinding of helix within the region of intercalation site found in crystal structure is the indirect evidences of these forces. We know that the overall situation in right handed nucleic acid can have different forms of sugar, and the sugar conformations in the backbone are highly flexible. Hence the orientation or geometrical descriptions of these models corresponding to minimum energy in fact exclude the sugar backbone torsion, and the geometrical pattern in the minimum structure may not exactly reproduce the crystal structure. Indeed there are several forces acting in crystal structures; crystal packing forces, the interaction with water molecules accumulated in grooves and effect from ions present in the crystal. However in general term, the differences in the stacking energies might be used for analyzing the relative change in the structure of various drug-sequence complexes that give some description of sequence specificity. In the present approach of defining sequence specificity, DFT method is not the right method but some intramolecular electron correlation is taken in the calculation, indeed intermolecular electron correlation is very important in such problem. It is hard to use MP2 level of theory with large basis set for large molecules and hence in some long range interactions occur in biological systems, the use of DFT is normally suggested. We have checked the variability of energies obtained from these methods and both the methods seem to locate the almost similar optimum structure. Hence the findings at least demonstrate the sequence preference chromophore intercalation of drug within sequences of DNA.

5.4 Conclusion

The following conclusion can be made from the study.

(1) The stacking energies of the azaacridine derivatives having N at different positions does not differ much. The stacking energies change with the position of N.

(2) Reasonable differences in stacking energy between the π– substituent stacking model and the π–π stacking are observed. In this case the stacking of π–π is more favourable than π–substituent stacking.

(3) Among the stacked models having acridine with substituents the stacking energies of GC-AZO8 (oxo) is the most favourable. In some cases there observed shifting of specificity from GC to AT.

The differences between the stacking energies obtained from different methods are significant. Even the DFT method can be applied for qualitative interpretation of sequence specificity.

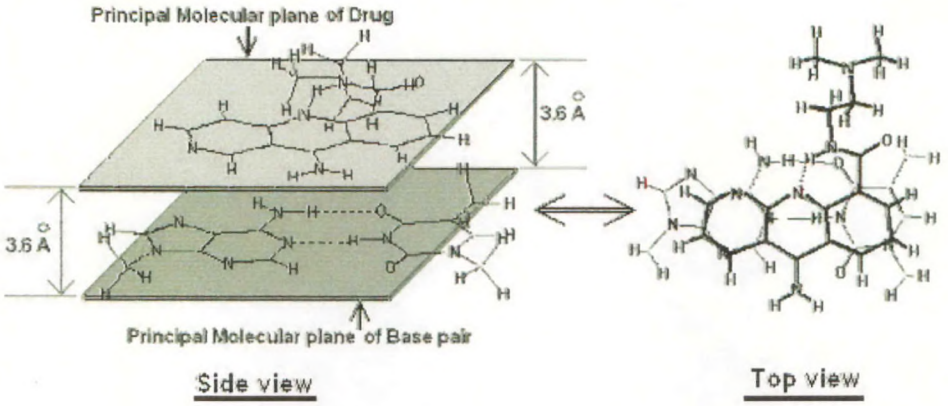

Figure 5.1 – Model of DNA base pair and drug stacking.

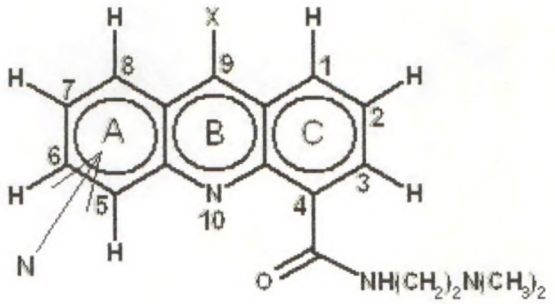

Figure 5.2 – General Structure of drug Azaacridine-4-carboxamide. AZA derivatives are formed by substituting N in to location 5, 6, 7 or 8. X= -CO, -NH_2, -Cl.

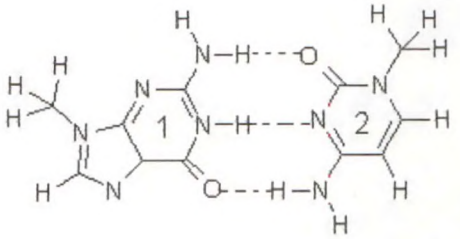

Figure 5.3 – GC Base pair.

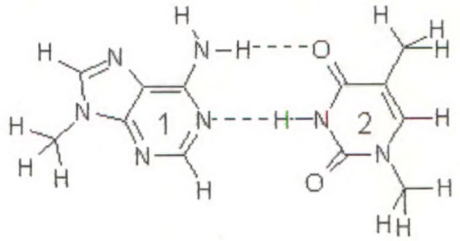

Figure 5.4 – AT Base pair.

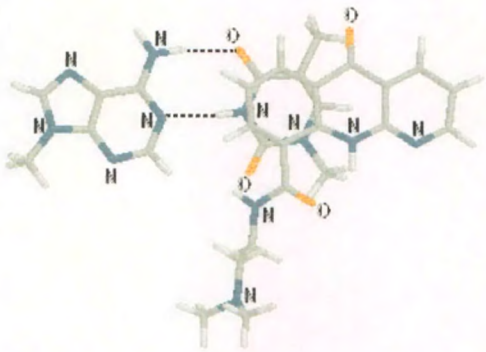

Figure 5.5a – Optimum AZO5-AT Stacking.

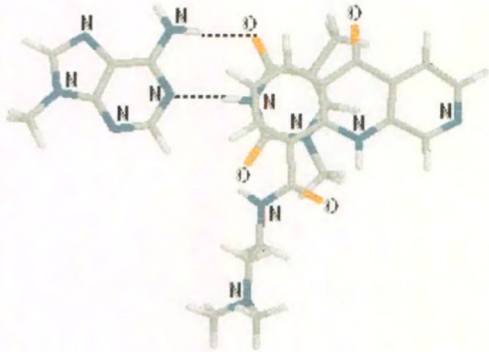

Figure 5.5b – Optimum AZO6-AT Stacking.

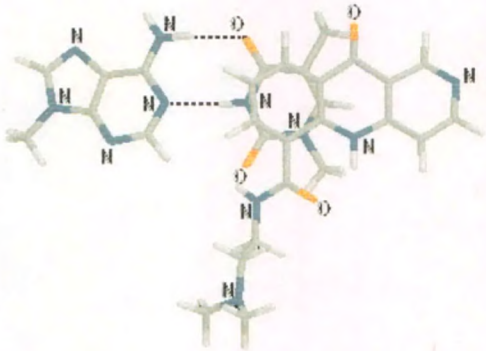

Figure 5.5c – Optimum AZO7-AT Stacking.

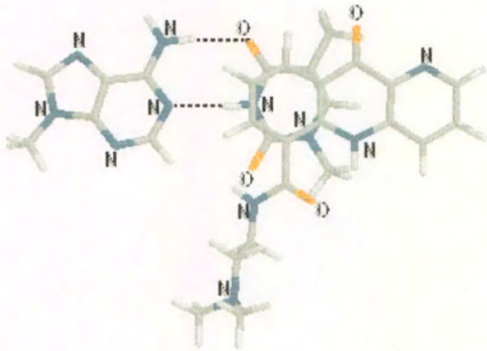

Figure 5.5d – Optimum AZO8-AT Stacking.

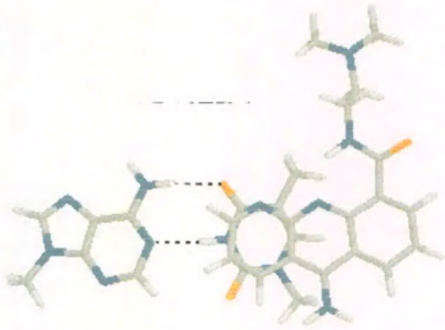

Figure 5.5e – Optimum AZN5-AT Stacking.

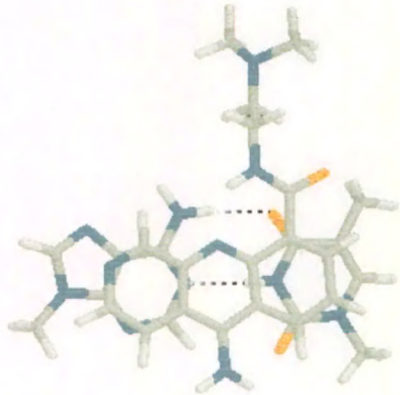

Figure 5.5f – Optimum AZN6-ATStacking.

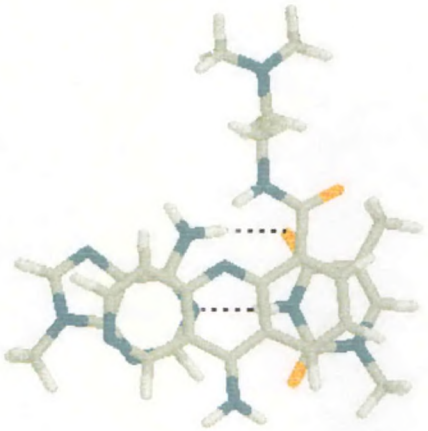

Figure 5.5g – Optimum AZN7-AT Stacking.

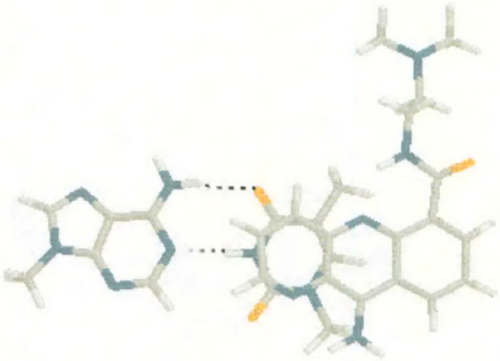

Figure 5.5h – Optimum AZN8-ATStacking.

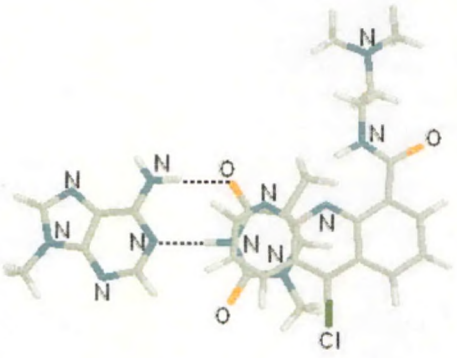

Figure 5.5i – Optimum AZCl5-AT Stacking.

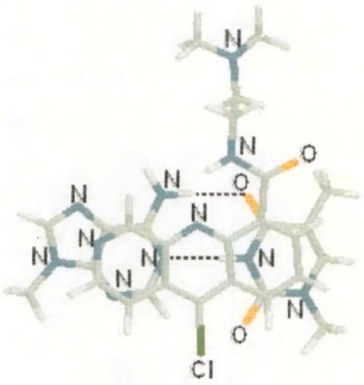

Figure 5.5j – Optimum AZCl6-AT Stacking.

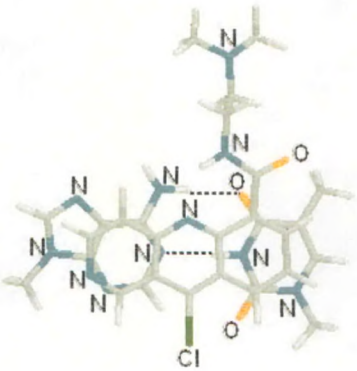

Figure 5.5k – Optimum AZCl7-AT Stacking.

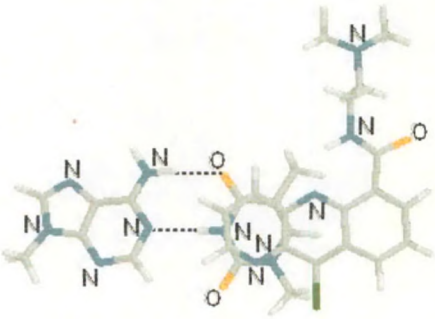

Figure 5.5l – Optimum AZCl8-AT Stacking.

Figure 5.5a-l – Optimum (π-π) stacking of AT and AZOx, AZNx and AZClx where x = 5, 6, 7 and 8.

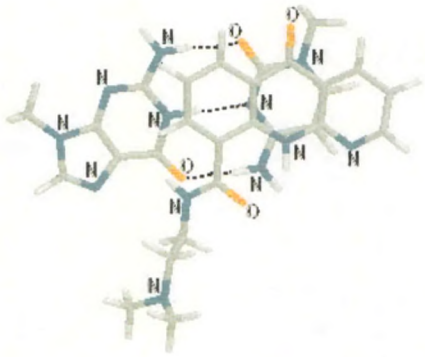

Figure 5.6a – Optimum AZO5-GC Stacking.

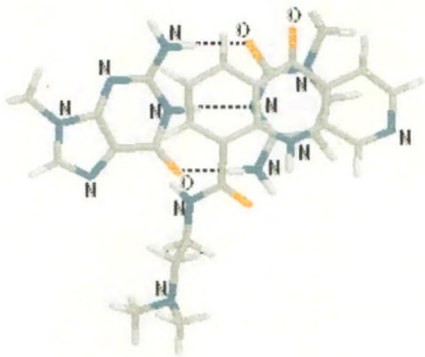

Figure 5.6b – Optimum AZO6-GC Stacking.

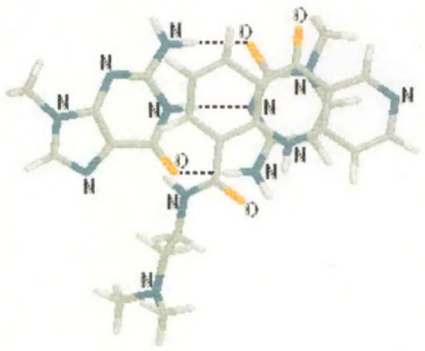

Figure 5.6c – Optimum AZO7-GC Stacking.

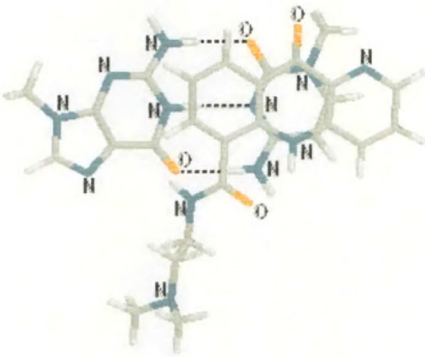

Figure 5.6d – Optimum AZO8-GC Stacking.

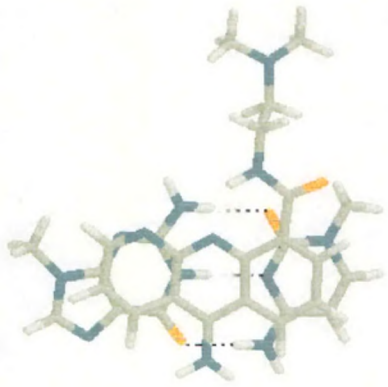

Figure 5.6e – Optimum AZN5-GC Stacking.

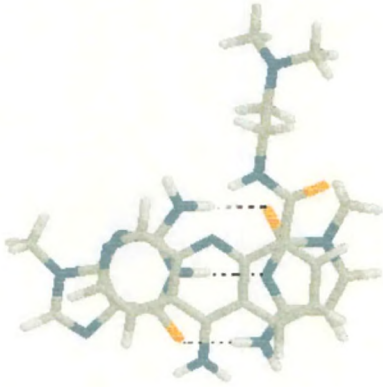

Figure 5.6f – Optimum AZN6-GC Stacking.

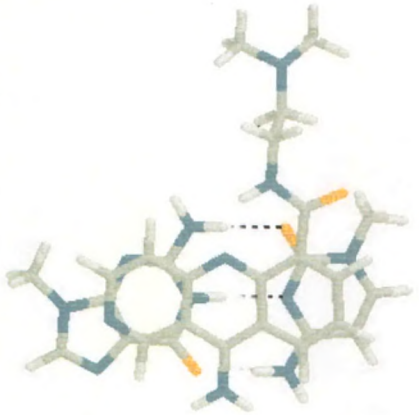

Figure 5.6g – Optimum AZN7-GC Stacking.

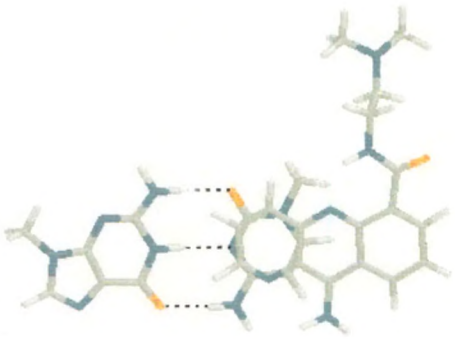

Figure 5.6h – Optimum AZN8-GC Stacking.

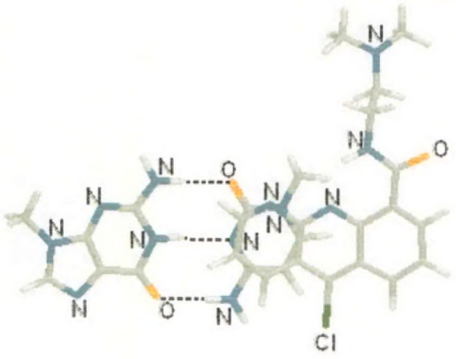

Figure 5.6i – Optimum AZCl5-AT Stacking.

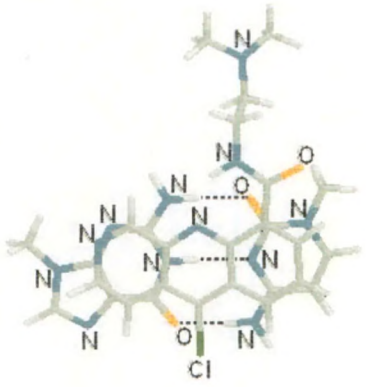

Figure 5.6j – Optimum AZCl6-AT Stacking.

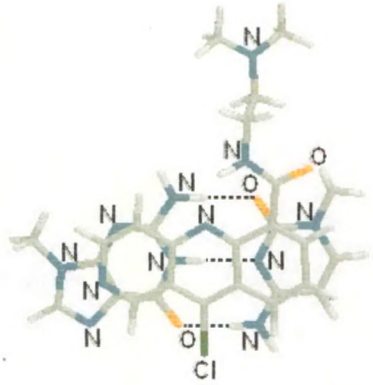

Figure 5.6k – Optimum AZCl7-AT Stacking.

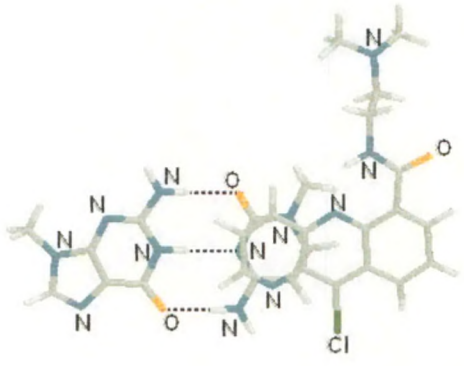

Figure 5.6l – Optimum AZCl8-AT Stacking.

Figure 5.6a - l – Optimum (π-π) stacking of GC and AZOx, AZNx and AZClx where x = 5, 6, 7 and 8.

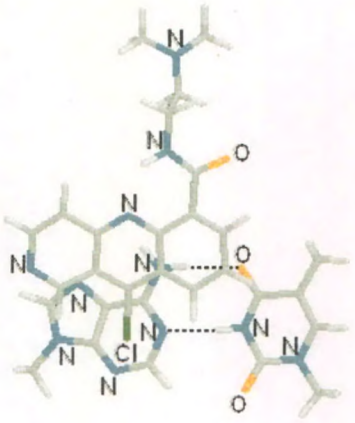

Figure 5.7a – Optimum AZCl7-AT Stacking.

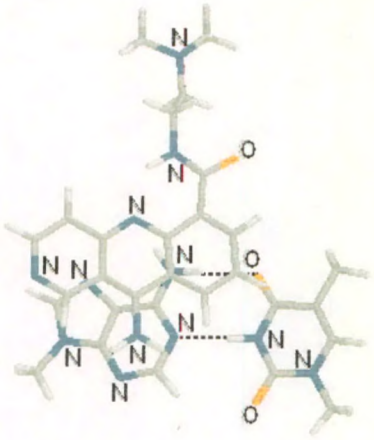

Figure 5.7b – Optimum AZN7-AT Stacking.

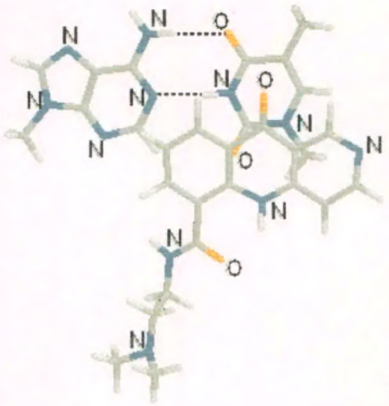

Figure 5.7c – Optimum AZO7-AT Stacking.

Figure 5.7a –c – Optimum (π-σ) stacking of AT base pair and AZOX, AZNX and AZClx where x= 5, 6, 7 and 8.

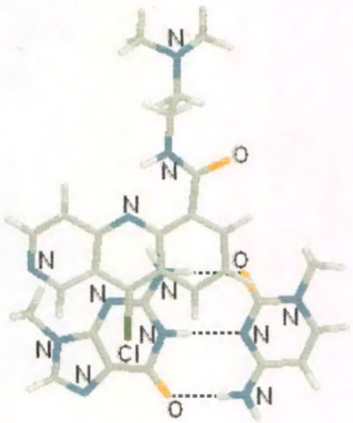

Figure 5.8a – Optimum AZCl7-GC Stacking.

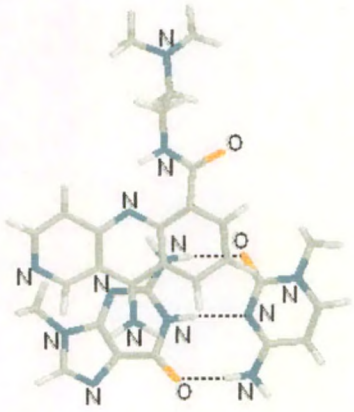

Figure 5.8b – Optimum AZN7-GC Stacking.

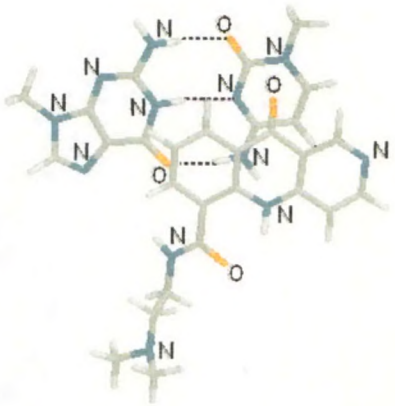

Figure 5.8c – Optimum AZO7-GC Stacking.

Figure 5.8a –c – Optimum (π-σ) stacking of GC base pair and AZOX, AZNX and AZClx where x = 5, 6, 7 and 8.

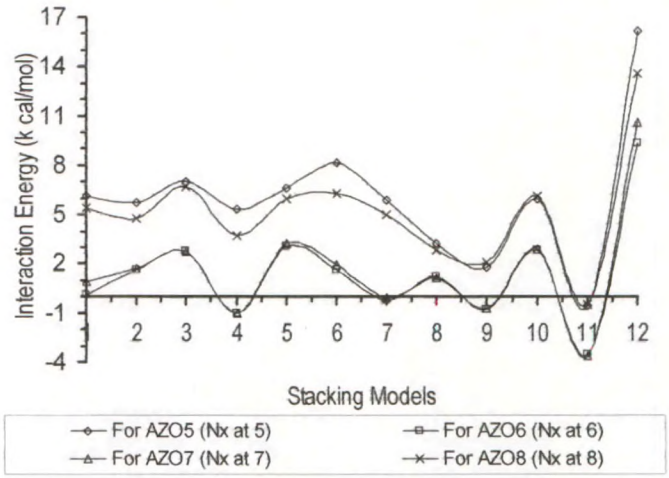

Figure 5.9a – Plot of stacking models versus variation of Interaction energies with different position of Nx for 9-oxoazaacridone-4-carboxamide (AZO) and AT stacking. (HF/6-31G)

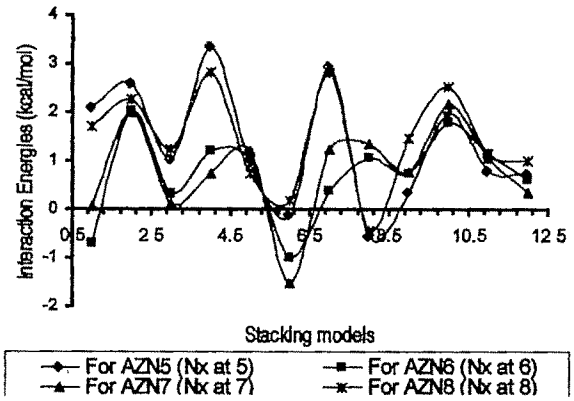

Figure 5.9b – Plot of stacking models versus variation of Interaction energies with different position of Nx for 9-aminoazaacridine-4-carboxamide (AZN) and AT stacking. (HF/6-31G)

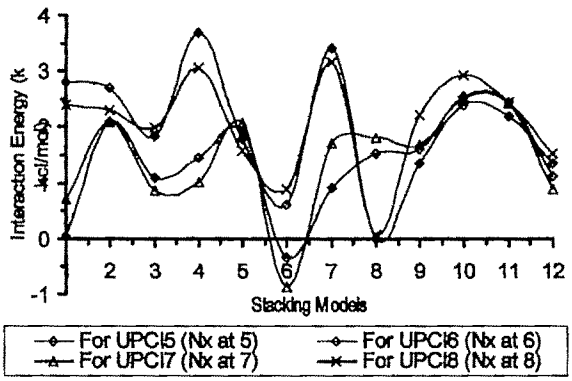

Figure 5.9c – Plot of stacking models versus variation of Interaction energies with different position of Nx for 9-chloroazaacridine-4-carboxamide (AZCl) and AT stacking. (HF/6-31G)

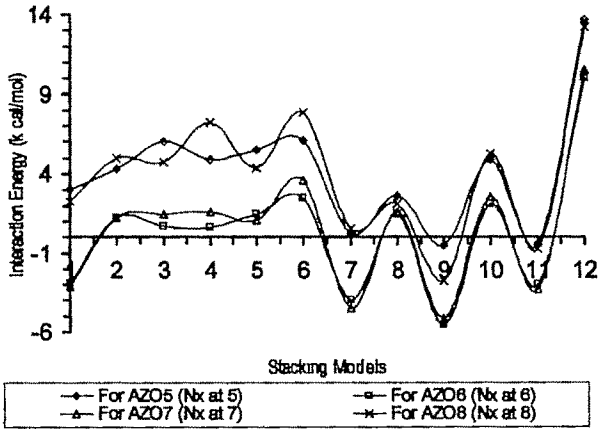

Figure 5.10a – Plot of stacking models versus variation of Interaction energies with different position of Nx for 9-ozoazaacridone-4-carboxamide (AZO) and GC stacking. (HF/6-31G)

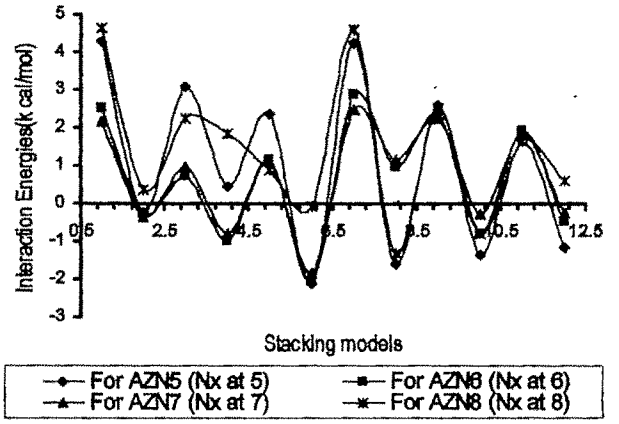

Figure 5.10b – Plot of stacking models versus variation of Interaction energies with different position of Nx for 9-aminoazaacridine-4-carboxamide (AZN) and GC stacking. (HF/6-31G)

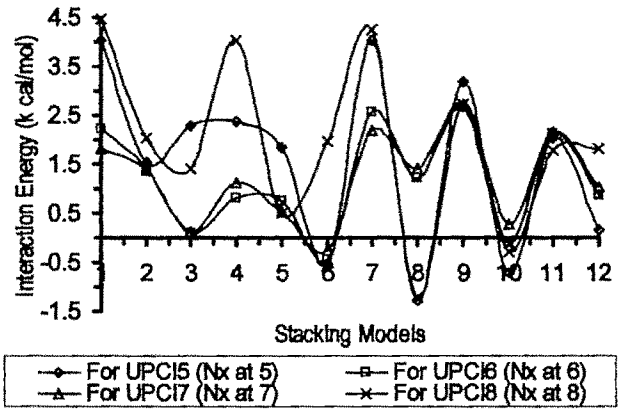

Figure 5.10c – Plot of stacking models versus variation of Interaction energies with different position of Nx for 9-chloroazaacridine-4-carboxamide (AZCl) and GC stacking. (HF/6-31G)

Table 5.1a – Construction of various stacking models (π - π stacking) of drugs and AT base pair.

Structure name (AT-DRGx-n)	Stacking location of Base pair	Stacking location of Drug
AT-DRGx-1	Ring-1	Ring-C (minor)
AT-DRGx-2	Ring-1	Ring-C (major)
AT-DRGx-3	Ring-1	Ring-B (minor)
AT-DRGx-4	Ring-1	Ring-B (major)
AT-DRGx-5	Ring-1	Ring-A (minor)
AT-DRGx-6	Ring-1	Ring-A (major)
AT-DRGx-7	Ring-2	Ring-A (minor)
AT-DRGx-8	Ring-2	Ring-A (major)
AT-DRGx-9	Ring-2	Ring-B (minor)
AT-DRGx-10	Ring-2	Ring-B (major)
AT-DRGx-11	Ring-2	Ring-C (minor)
AT-DRGx-12	Ring-2	Ring-C (major)

DRG = name of the drug; x = position of Nx; n = stacking location; (minor) = minor groove; (major) = major groove. (Drugs are a. 9-oxoazaacridone-4-carboxamide (AZO), b. 9-aminoazaacridine-4-carboxamide (AZN) and c. 9-chloroazaacridine-4-carboxamide (AZCl)

Table 5.1b – Construction of various stacking models (π - π stacking) of drugs and GC base pair.

Structure name (GC-DRGx-n)	Stacking location of Base pair	Stacking location of Drug
GC-DRGx-1	Ring-1	Ring-C (major)
GC-DRGx-2	Ring-1	Ring-C (minor)
GC-DRGx-3	Ring-1	Ring-B (major)
GC-DRGx-4	Ring-1	Ring-B (minor)
GC-DRGx-5	Ring-1	Ring-A (major))
GC-DRGx-6	Ring-1	Ring-A (minor)
GC-DRGx-7	Ring-2	Ring-A (major)
GC-DRGx-8	Ring-2	Ring-A (minor)
GC-DRGx-9	Ring-2	Ring-B (major)
GC-DRGx-10	Ring-2	Ring-B (minor)
GC-DRGx-11	Ring-2	Ring-C (major)
GC-DRGx-12	Ring-2	Ring-C (minor)

DRG = name of the drug; x = position of Nx; n = stacking location; (minor) = minor groove; (major) = major groove. (Drugs are a. 9-oxoazaacridone-4-carboxamide (AZO), b. 9-aminoazaacridine-4-carboxamide (AZN) and c. 9-chloroazaacridine-4-carboxamide (AZCl)

Table 5.1c – Modeling scheme for Stacking of substituents and base pair Stacking.

Structure name (XX-DRGx-n)	Stacking location of Base pair	Stacking location of Drug
AT-DRGx-S1	Ring-2	substituents at C9 (minor)
AT-DRGx-S2	Ring-2	substituents at C9 (major)
AT-DRGx-S3	Ring-1	substituents at C9 (minor)
AT-DRGx-S4	Ring-1	substituents at C9 (major)
GC-DRGx-S1	Ring-2	substituents at C9 (major)
GC-DRGx-S2	Ring-2	substituents at C9 (minor)
GC-DRGx-S3	Ring-1	substituents at C9 (major)
GC-DRGx-S4	Ring-1	substituents at C9 (minor)

XX= AT or GC; DRG = name of the drug; x = position of Nx; n = stacking location; (minor) = minor groove; (major) = major groove. (Drugs are a. 9-oxoazaacridone-4-carboxamide (AZO), b. 9-aminoazaacridine-4-carboxamide (AZN) and c. 9-chloroazaacridine-4-carboxamide (AZCl)

Table 5.2 – The computed Interaction energies of AZO, AZN and AZCl with Nx at different position and AT base pair. (in k cal/mol)

AT-AZO stacking (AT-AZOx-n)		AT-AZN stacking (AT-AZNx-n)		AT-AZCl stacking (AT-AZClx-n)	
Optimum structure	Interaction energies	Optimum structure	Interaction energies	Optimum structure	Interaction energies
AT-AZO5-11	-0.501	AT-AZN5-8	-0.554	AT-AZCl5-8	-0.007
AT-AZO6-11	-3.479	AT-AZN6-6	-0.995	AT-AZCl6-6	-0.328
AT-AZO7-11	-3.571	AT-AZN7-6	-1.531	AT-AZCl7-6	-0.882
AT-AZO8-11	-0.483	AT-AZN8-8	-0.431	AT-AZCl8-8	0.075

x = position of Nx; n = stacking location. (Drugs are 9-oxoazaacridone-4-carboxamide (AZO), 9-aminoazaacridine-4-carboxamide (AZN) and 9-chloroazaacridine-4-carboxamide (AZCl))

Table 5.3 – The computed Interaction energies of AZO, AZN and AZCl with Nx at different position and GC base pair. (in k cal/mol)

GC-AZO stacking (GC-AZOx-n)		GC-AZN stacking (GC-AZNx-n)		GC-AZCl stacking(GC-AZClx-n)	
Optimum structure	Interaction energies	Optimum structure	Interaction energies	Optimum structure	Interaction energies
GC-AZO5-9	-0.537	GC-AZN5-6	-2.132	GC-AZCl5-8	-1.282
GC-AZO6-9	-5.517	GC-AZN6-6	-2.078	GC-AZCl6-6	-0.448
GC-AZO7-9	-5.196	GC-AZN7-6	-1.834	GC-AZCl7-6	-0.236
GC-AZO8-9	-2.788	GC-AZN8-8	-1.336	GC-AZCl8-8	-1.215

x = position of Nx; n = stacking location. (Drugs are a. 9-oxoazaacridone-4-carboxamide (AZO), b. 9-aminoazaacridine-4-carboxamide (AZN) and c. 9-chloroazaacridine-4-carboxamide (AZCl))

Table 5.4a – Variation of Net Charge on Nx of optimum stacked structure of AT and 9-aminoazaacridine-4-carboxamide (AZN).

Optimum Stacked Structure (AT-AZNx-n)	Total Atomic Charge on Nx	
	Free Drug	Interacted Drug
AT- AZN5-8	-0.525	-0.530
AT- AZN6-6	-0.513	-0.520
AT- AZN7-6	-0.552	-0.565
AT- AZN8-8	-0.584	-0.587

p = position of Nx; n = stacking location

Table 5.4b – Variation of Net Charge on Nx of optimum stacked structure of GC and 9-aminoazaacridine-4-carboxamide (AZN).

Optimum Stacked Structure (GC-AZNx-n)	Total Atomic Charge on Nx	
	Free Drug	Interacted Drug
GC- AZN5-6	-0.525	-0.533
GC- AZN6-6	-0.513	-0.515
GC- AZN7-6	-0.552	-0.562
GC- AZN8-8	-0.584	-0.592

p = position of Nx; n = stacking location.

Table 5.5a – Variation of Net Charge on Nx of optimum stacked structure of AT and 9-oxoazaacridone-4-carboxamide (AZO).

Optimum Stacked Structure (AT-AZOx-n)	Total Atomic Charge on Nx	
	Free Drug	Interacted Drug
AT-AZO5-11	**-.587**	-0.568
AT-AZO6-11	**-.486**	-0.485
AT-AZO7-11	**-.543**	-0.542
AT-AZO8-11	**-.490**	-0.478

p = position of Nx; n = stacking location

Table 5.5b – Variation of Net Charge on Nx of optimum stacked structure of GC and 9-oxoazaacridone-4-carboxamide (AZO).

Optimum Stacked Structure (GC-AZOx-n)	Total Atomic Charge on Nx	
	Free Drug	Interacted Drug
GC-AZO5-9	**-.587**	-0.571
GC-AZO6-9	**-.486**	-0.488
GC-AZO7-9	**-.543**	-0.547
GC-AZO8-9	**-.490**	-0.484

p = position of Nx; n = stacking location

Table 5.6a – Variation of Net Charge on Nx of optimum stacked structure of AT and 9-chloroazaacridine-4-carboxamide (AZCl) stacking.

Optimum Stacked Structure (AT-AZOx-n)	Total Atomic Charge on Nx	
	Free Drug	Interacted Drug
AT-AZCl5-8	**-.511**	-0.516
AT-AZCl6-6	**-.516**	-0.524
AT-AZCl7-6	**-.537**	-0.549
AT-AZCl8-8	**-.531**	-0.535

p = position of Nx; n = stacking location

Table 5.6b – Variation of Net Charge on Nx of optimum stacked structure of GC and 9-chloroazaacridine-4-carboxamide (AZCl) stacking.

Optimum Stacked Structure (GC-AZOx-n)	Total Atomic Charge on Nx	
	Free Drug	Interacted Drug
GC-AZCl5-8	**-.511**	-0.521
GC-AZCl6-6	**-.516**	-0.518
GC-AZCl7-6	**-.537**	-0.545
GC-AZCl8-8	**-.531**	-0.541

p = position of Nx; n = stacking location

Table 5.7a – The computed Interaction Energies of the optimum stacked models of 9-oxoazaacridone-4-carboxamide (AZO) and AT base pair at different level of theory.

Stacking Geometry (AT-AZOx-n)	Observed binding direction	Interaction energies (In k cal/mol)			
		HF/ 6-31G*	HF/ 6-31G**	B3LYP/ 6-31G**	MP2/6-31G (stacked portion)
AT-AZO5-11	Major groove	-6.285	-6.281	-3.861	-5.610
AT-AZO6-11	Major groove	-3.225	-3.234	-4.432	22.979
AT-AZO7-11	Major groove	-3.3451	-3.361	-4.528	-11.257
AT-AZO8-11	Major groove	-6.2817	-6.267	-3.506	-5.371

p = position of Nx; n = stacking location.

Table 5.7b – The computed Interaction Energies of the optimum stacked models of 9-aminoazaacridine-4-carboxamide (AZN) and AT base pair at different level of theory.

Stacking Geometry (AT-AZNx-n)	Observed binding direction	Interaction energies (In k cal/mol)			
		HF/ 6-31G*	HF/ 6-31G**	B3LYP/ 6-31G**	MP2/6-31G (stacked portion)
AT-AZN5-8	Major groove	-0.684	-0.717	-1.412	-9.419
AT-AZN6-6	Major groove	-0.908	-0.942	-2.271	-10.160
AT-AZN7-6	Major groove	-1.493	-1.524	-2.813	-10.530
AT-AZN8-8	Major groove	-0.621	-0.649	-1.284	-7.817

p = position of Nx; n = stacking location.

Table 5.7c – The computed Interaction Energies of the optimum stacked models of 9-chloroazaacridine-4-carboxamide (AZCl) and AT base pair at different level of theory.

Stacking Geometry (AT-AZClx-n)	Observed binding direction	Interaction energies (In k cal/mol)			
		HF/ 6-31G*	HF/ 6-31G**	B3LYP/ 6-31G**	MP2/6-31G (stacked portion)
AT-AZCl5-8	Major groove	-0.184	-0.200	-0.990	-16.910
AT-AZCl6-6	Major groove	-0.349	-0.374	-1.536	-10.119
AT-AZCl7-6	Major groove	-0.919	-0.949	-2.009	-10.436
AT-AZCl8	As all interaction have positive value higher basis sets not done.				

p = position of Nx; n = stacking location.

Table 5.8a – The computed Interaction Energies of the optimum stacked models of 9-oxoazaacridone-4-carboxamide (AZO) and GC base pair at different level of theory.

Stacking Geometry (GC-AZOx-n)	Observed binding direction	Interaction energies (In k cal/mol)			
		HF/ 6-31G*	HF/ 6-31G**	B3LYP/ 6-31G**	MP2/6-31G (stacked portion)
GC-AZO5-9	Major groove	-6.931	-6.882	-5.648	-7.948
GC-AZO6-9	Major groove	-5.604	-5.611	-7.095	-7.780
GC-AZO7-9	Major groove	-5.293	-5.291	-7.097	-7.920
GC-AZO8-9	Major groove	**-8.830**	**-8.797**	**-6.502**	-7.698

p = position of Nx; n = stacking location.

Table 5.8b – The computed Interaction Energies of the optimum stacked models of 9-aminoazaacridine-4-carboxamide (AZN) and AT base pair at different level of theory.

Stacking Geometry (GC-AZNx-n)	Observed binding direction	Interaction energies (In k cal/mol)			
		HF/6-31G*	HF/6-31G**	B3LYP/6-31G**	MP2/6-31G (stacked portion)
GC-AZN5-6	Minor groove	-2.213	-2.277	-3.850	-7.352
GC-AZN6-6	Minor groove	-1.990	-2.058	-3.766	-8.115
GC-AZN7-6	Minor groove	-1.866	-1.942	-3.522	-7.274
GC-AZN8-8	Minor groove	-1.415	-1.419	-1.638	-7.969

p = position of Nx; n = stacking location .

Table 5.8c – The computed Interaction Energies of the optimum stacked models of 9-aminoazaacridine-4-carboxamide (AZN) and AT base pair at different level of theory.

Stacking Geometry (GC-AZClx-n)	Observed binding direction	Interaction energies (In k cal/mol)			
		HF/6-31G*	HF/6-31G**	B3LYP/6-31G**	MP2/6-31G (stacked portion)
GC-AZCl5-8	Minor groove	-1.448	-1.466	-1.940	-17.743
GC-AZCl6-6	Minor groove	-0.560	-0.601	-2.420	-7.875
GC-AZCl7-6	Minor groove	-0.445	-0.494	-2.009	-8.222
GC-AZCl8-8	Minor groove	-1.385	-1.399	-1.718	-8.004

p = position of Nx; n = stacking location

Table 5.9 – The computed Interaction Energies of the optimum stacked models of C9 substituent of AZO's, AZN's and AZCl's with AT base pair at different level of theory.

Stacking Geometry (AT-DRGx-n)	Observed binding direction	Interaction energies (In k cal/mol)		
		HF/6-31G*	HF/6-31G**	B3LYP/6-31G**
AT-AZO7-S2	Major groove	-1.934	-1.842	-1.859
AT-AZN7-S4	Major groove	-1.162	-1.157	-1.193
AT-AZCl7-S4	Major groove	-0.219	-0.114	-0.136

DRG = name of the drug; p = position of Nx; n = stacking location

Table 5.10 – The computed Interaction Energies of the optimum stacked models of C9 substituent of AZO's, AZN's and AZCl's with GC base pair at different level of theory.

Stacking Geometry (GC-DRGx-n)	Observed binding direction	Interaction energies (In k cal/mol)		
		HF/6-31G*	HF/6-31G**	B3LYP/6-31G**
GC-AZO7-S1	Major groove	-5.704	-5.079	-5.072
GC-AZN7-S4	Major groove	-2.703	-2.800	-2.820
GC-AZCl7-S4	Major groove	-0.631	-0.604	-0.618

DRG = name of the drug; p = position of Nx; n = stacking location

Reference

1. Baguley B C, Denny W A, Atwell G J, Cain B F, *J Med Chem*, **1981**, 24, 170.
2. Wright R D McR, Wakelin L P G, Fields A, Acheson R M, Waring M J, *Biochemistryl*, **1980**, 19, 5825.
3. Finlay G F, Baguley B C, *J Cancer Clin Oncol*, **1984**, 20, 947.
4. Finlay G J, Baguley B C, *Eur J Cancer Clin Oncol*, **1984**, 20, 947.
5. Showalter H D H, Johnson J L, Werbel L M, Leopold W R, Jackson R C, Elslager E F, *J Med Chem*, **1984**, 27, 253.
6. Bowden G T, Roberts R, Alberts D S, Peng Y M, Garcia D, *Cancer Res*, **1985**, 45, 4915.
7. Atwell G J, Cain B F, Baguley B C, Finlay G J, Denny W A, *J Med Chem*, **1984**, 27, 1481.
8. Rewcastle G W, Denny W A, *Synthesis*, **1985**, 217.
9. Rewcastle G W, Denny W A, *Synthesis*, **1985**, 220.
10. Denny W A, Atwell G J, Rewcastle G W, Baguley B C, *J Med Chem*, **1987**, 30, 658-663.
11. Atwell G J, Rewcastle G W, Baguley B C, Denny W A, *J Med Chem*, **1987**, 30, 664-669.
12. Finlay G J, Marshall E S, Matthews J H L, Paull K D, Baguley B C, *Cancer Chemother Pharmacol*, **1993**, 31, 404-406.
13. Haldane A, Finlay G J, Gavin J B, Baguley B C, *Cancer Chemother Pharmacol*, **1992**, 29, 475-479.
14. Palmer B D, Rewcastle G W, Baguley B C, Denny W A, *J Med Chem*, **1988**, 31, 707-712.
15. Wakelin L P G, Atwell G J, Rewcastle G W, Denny W A, *J Med Chem*, **1987**, 30, 855-862.
16. Wilson W R, Anderson R F, Denny W A, *J Med Chem*, **1989**, 32, 23-30.
17. Hunter C A, *J Mol Biol*, **1993**, 230, 1025.

18.(a) Hrouda V, Florian J, Hobza P, *J Phys Chem*, **1993**, 97, 1542.

(b) Gould I R, Kollman P A, *J Am Chem Soc*, **1994**, 116, 2493.

(c) Sponer J, Leszezynski J, Hobza P, *J Phys Chem*, **1996**, 100, 1965.

(d) Sponer J, Hobza P, *J Am Chem Soc*, **1994**, 116, 709.

(e) Sponer J, Hobza P, *J Biomol Struct Dyn*, **1994**, 11, 1357.

19 Frisch M J, Trucks G W, Schlegel H B, Gill P M W, Johnson B G, Robb M A, Cheeseman J R, Keith T, Petersson G A, Montgomery J A, Raghavachari K, Al-Laham, M A, Zakrzewaki V G, Ortiz J V, Foresmann J B, Ciolowski J, Stefanov B B, Namayakkara A, Challacombe M, Peng C Y, Ayala P Y, Chen W, Wong M W, Andres J L, Replogle E S, Gomperts R, Martin R L, Fox D J, Binkley J S, Defrees D J, Baker J, Stewart J P, Head-Gordon M, Gonzalez C & Pople J A, Gaussian 94; Gaussian Inc, Pittsburgh PA, **1995**.